

<https://doi.org/10.15407/knit2023.03.119>

**D. ELFIKY\***<sup>1</sup>, Head of structural, thermal, space Environment Dept. Space Science Div., Ass. Prof.

ORCID: 0000-0003-4772-667X

E-mail: delfiky@narss.sci.eg

**S. AZIZ**<sup>1</sup>, RA on structural, thermal, space Environment Dept. Space Science Div., MSc

E-mail: sara.ramadan.aiz93@gmail.com\*, sara.ramadan@narss.sci.eg\*

**N. HESHAM**<sup>1</sup>, RA on structural, thermal, space Environment Dept. Space Science Div., Bsc

E-mail: nourhanhesham531@gmail.com

**A. AYMAN**<sup>2</sup>, Head of Payload Dept., PhD

E-mail: ayman.ahmed@moonvillageassociation.org

<sup>1</sup> National Authority for Remote Sensing and Space Science (NARSS)

23-josef-tito, new nozha, Cairo 11769, Egypt

<sup>2</sup> Egyptian Space Agency, Cairo, Egypt

\*Corresponding author

## LOW COST DOSIMETER MODULE FOR MVA LUNAR LANDER MISSION

*Understanding the lunar radiation environment is crucial for future space exploration missions, as the lack of atmospheric and magnetic shielding allows charged particles of varying energies and origins to penetrate the surface of the moon. In space radiation environments, it is common practice to use radiation dosimeters to measure absorbed dose and dose rate.*

*In this study, the payload will include a radiation dosimeter capable of measuring the radiation intensity at the landing site's surface. The design concept and implementation of a radiation readout system for the real-time measurement of gamma absorbed dose and dose rate at the surface of the landing area for the MVA mission are based on a photodiode sensor that is commercially available and will be used as a gamma radiation sensor. The module experienced low levels of activity (Cs<sup>137</sup>, Co<sup>60</sup>, and Sr<sup>90</sup>). The performance of the photodiode-based module has been demonstrated by the Giger counter. Due to its low cost and high sensitivity, this radiation module would be clearly advantageous.*

**Keywords:** Lunar lander, Radiation dosimeter, photodiode sensor, TIA.

### 1. INTRODUCTION

Future space research missions require a comprehensive knowledge of the lunar radiation environment, as the lack of air and magnetic shielding allows charged particles of varying energies and origins to penetrate the lunar surface [3]. In space radiation conditions, the measurement of absorbed dosage and dose rate is a routine duty; this is achieved with equipment known as radiation dosimeters [7]. Using a multi-national team approach, different partners working on

the payload system modules of the MVA lunar lander will create an image system for the MVA payload lunar lander. System aims include getting a live stream of the Earth from the Moon, detecting radiation dosage and earthquakes on the Moon's surface and transmitting this data back to Earth via satellite for the purpose of gathering scientific data, those sensors will be put on the platform in question. The radiation sensor module is being developed by the National Authority for Remote Sensing and Space Science,

Цитування: Elfiky D., Aziz S., Hesham N., Ayman A. Low Cost Dosimeter Module for MVA Lunar Lander Mission. *Space Science and Technology*. 2023. 29, № 4 (143). P. 119–126. <https://doi.org/10.15407/knit2023.03.119>

© Publisher ПН «Академперіодика» of the NAS of Ukraine, 2023. This is an open access article under the CC BY-NC-ND license (<https://creativecommons.org/licenses/by-nc-nd/4.0/>)

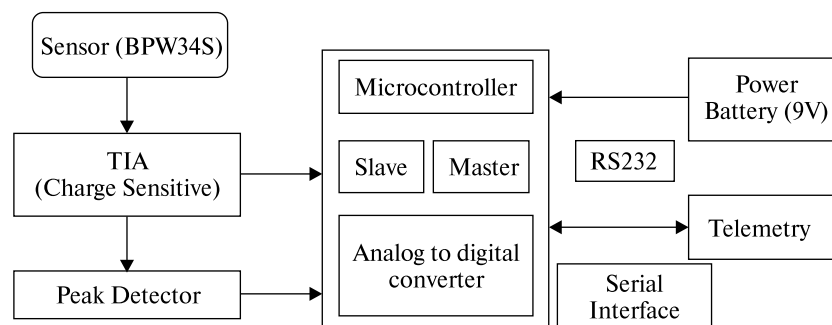


Figure 1. Design concept of the radiation dosimeter readout module

which is a joint partner. In this project, the camera will have a radiation dosimeter that can measure the radiation intensity at the surface of the landing area. The radiation dosimeter data will be translated into “sound signals”, which can be used as an exciting effect with the image to create more publicity: “You can hear and see the lunar surface!” The device will detect gamma in the 10 keV — 1 MeV energy range using a low-cost photodiode sensor. This radiation module is an obvious winner due to its low cost and high sensitivity. PIN photodiodes have been used in a variety of works to detect radiation directly without the use of an expensive low-noise charge preamplifier [5, 6]. Low leakage photodiodes with entry windows that are thin enough to enable gamma radiation to pass through to the depletion zone have shown sufficient energy resolution to be connected to inexpensive preamplifiers for gamma radiation. Accordingly, there is a need for a low-cost, portable, and adaptable amplifier that could be attached to the detector. The most significant quality of the amplifier in such an application is not the energy resolution but the noise discrimination, because the detector will be utilized as a particle counter. We employed three PIN photodiodes in our design to enhance the active area of the sensor and, hence, minimize decimation noise.

## 2. METHODOLOGY

**2.1. Sensor Selection.** Due to its tiny sensitivity region, the PIN photodiode is an ideal radiation detector for our experiments. It’s simple to identify signals from tiny samples because the cosmic ray background is so low [4]. Bpw34s PIN photodiodes may be used to detect gamma rays that travel through its depletion

layer and form numerous electron-hole pairs. When the diode is reverse-biased, virtually all of the charge carriers will be driven away, resulting in a tiny current pulse that can be amplified and processed [8]. Because the photodiode’s output signal has such a small amplitude, an instrumentation amplifier circuit with extremely low noise is required. Light must be fully eliminated when using a photodiode as a detector of gamma radiation because else the photocurrent would overwhelm the signal we are looking for [9].

**2.2. Design Concept.** Bpw34s, a commercially available PIN photodiode, has been used in this work to evaluate a small and unique dosimeter device. The concept of functioning is dependent on the electrical properties of the sensor being changed by radiation (i.e. the change of current flowing through the sensor or the voltage across the sensor). Because of their tiny size and inherent sensitivity to ionizing radiation, photodiodes are frequently employed as radiation sensors. From Pico-ampere to Micro-ampere, the photodiode’s output signal is a current. The output current is so little that it can’t be picked up by the sensor. As a result, the output signal must be amplified and the current converted into a proportional voltage using the Transimpedance amplifier TIA technique [10]. In order to digitize the TIA output voltage signals, there is always a trade-off between hardware resources, expenses, and space and power consumption when selecting a conversion approach. To capture the TIA’s output in digital signal processing (DSP), high-speed ADCs with sampling rates of up to 500,000 samples per second (sps) are used. The light detector’s output is digitized directly at even greater rates (> 250 Msps) in another digital technique. Pulse shape discrimina-

tion, for example, necessitates the use of high-rate digitization to capture temporal pulse shape information. Analog pulse height can't be reliably calculated since the sampling time is so sluggish compared to the light pulse width. Using a peak detector (PKD) [2], a well-known analogue circuit that can convert transient voltage pulse heights into permanent voltage [1], is the best approach in this scenario. Serial Interface will receive the output data through RS232 and forward it to the destination. Fig. 1 depicts the circuit's overall design idea.

We chose the TL082 for TIA and LM358 for PDK for such design (2 pF) because of its excellent combination of low bias current, offset voltage, power consumption, and wide bandwidth with feedback resistor (50 k) and feedback capacitor.

The ATmega328-based Arduino Nano is a small, complete, and breadboard-friendly board (Arduino Nano 3.x). The Arduino Nano is organized using the Arduino (IDE), which is available for a variety of platforms. IDE is an abbreviation for Integrated Development Environment. An accurate clock frequency is generated using an Arduino Nano.

**2.3. The System Simulation Model.** In general, there are three major steps for simulating the sensor readout board. Firstly, simulation of the photodiode output by a two-diode model Secondly, the transient impedance amplification (TIA) circuit, which works as a pre-amplifier for the signal produced by the photodiode. Finally, the peak detector PKD circuit counts the signal, which converts the transient voltage pulse heights into persistent voltages. The final output will be the input of the microcontroller, where microcontroller is used to count the detected signals. The simulation model of the sensor board is shown in Fig. 2. Simulation of the photodiode (Bpw34s) depends on simulating the maximum output of the dark current in dark condition when the photodiode is reverse biased with 9 V. The output current of the photodiode is ( $I_{pd}$ ) the current output of the photodiode that connected between the ground and the inverting input of the op-amp, it is approximately 70  $\mu$ A as shown in Fig. 2. The design of the Transimpedance amplifier (TIA) process presented  $C_f$  and  $R_f$  are the feedback resistor ( $R_1$ ) and feedback capacitor ( $C_1$ ) respectively. The peak detector (PKD) circuit was used to remove the voltage drop across the diode.

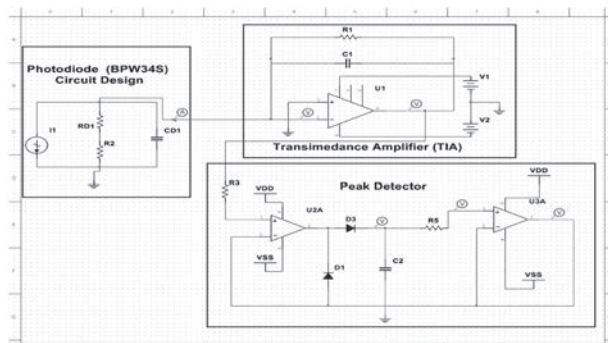


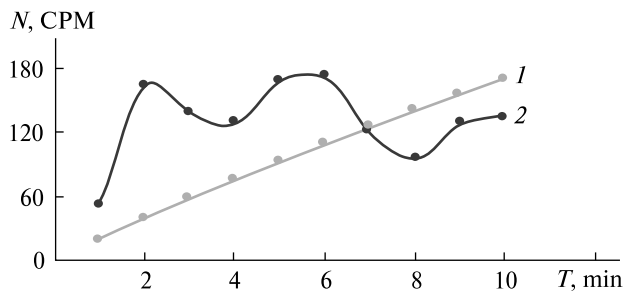
Figure 2. The system simulation model of the gamma radiation readout module

Table 1. Radiation Sources

| Source                    | Energy   | Activity    |
|---------------------------|----------|-------------|
| Co <sup>60</sup> (gamma)  | 2.8 MeV  | 1.0 $\mu$ C |
| Sr <sup>90</sup> (beta)   | 1.17 MeV | 10 $\mu$ C  |
| Co <sup>60</sup> (gamma)  | 1.3 MeV  | 2.8 mC      |
| Cs <sup>137</sup> (gamma) | 662 keV  | 1 mC        |

**2.4. Software Overview.** The main task of the software design is controlling the microcontroller to count the output signals in response to the radiation levels that pass through the photodiode to ensure an accurate counting result. Once the circuit is powered, the pulses are received by the microcontroller according to the radiation dose and counted; then, with an easy calculation, we can get the value of the radiation. The analog signal output of the (PKD) with pulse width is 250 microseconds and pulse height is 0–5 V is received by analog pin A1 of microcontroller. This pin works as ADC, so the signal converted to digital signal in range to 0–1024. This value compared with lowest level of volt induced by photodiodes when exposed to radiation sources. If the value is greater than threshold value the counter will start to count. The code we use for the board is counting pulses every one minutes. So we get the number of pulses by minute (CPM), then, according to the photodiode documentation we divide (CPM) by the conversion factor of the photodiode (0.0057) and we have the value of radiation in  $\mu$ SV/h.

**2.5. The System Testing.** The sensor board must be tested by exposing the board to different types of



**Figure 3.** The reading of Bpw34s board (line 1) and Geiger counter (line 2) after irradiation to  $\text{Co}^{60}$  with activity  $1 \mu\text{C}$  ( $E = 2.8 \text{ MeV}$ )

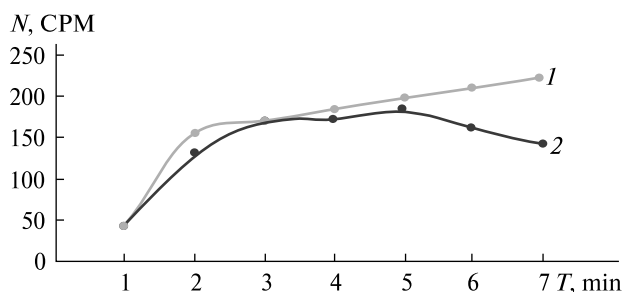


**Figure 4.** The reading of the board (line 1) and Geiger counter (line 2) after irradiation to  $\text{Sr}^{90}$  with activity  $10 \mu\text{C}$  ( $E = 1.17 \text{ MeV}$ )

radiation, and compare the result of the system with the Geiger counter, the testing was done at Helwan university labs. Three radiation sources were chosen to the irradiation process are  $\text{Cs}^{137}$ ,  $\text{Co}^{60}$ , and  $\text{Sr}^{90}$ . The radiation sources and its activity is shown in Table 1.

Appendix 1 includes the Figures, which demonstrate a) prototype of the sensor board, b) the schematic design of the sensor board, c) final 3D design of the sensor board, and d) mechanical structure of the aluminum box.

### 3. RESULT AND DISCUSSION

**3.1. Simulation Model.** Firstly, the result of the simulation model of the photodiode circuit shown at left of according to the photodiode characterization as “photodiode Bpw34s circuit Design”, the circuit simulated by current source in range of ( $1 \mu\text{A}$  to  $70 \mu\text{A}$ ) according to the amount of dark current corresponding to reverse bias, shunt resistance ( $5 \text{ M ohm}$ ) and photodiode capacitance ( $30 \text{ pF}$ ) simulate the shunts inside the photodiode. Secondly, operational ampli-

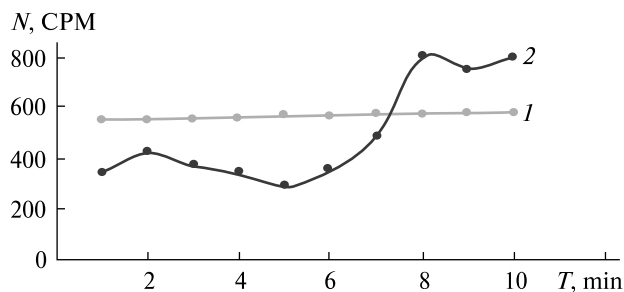


**Figure 5.** The reading of the board (line 1) and Geiger counter (line 2) after irradiation to  $\text{Cs}^{137}$  with activity  $1 \text{ mC}$  ( $E = 662 \text{ keV}$ )

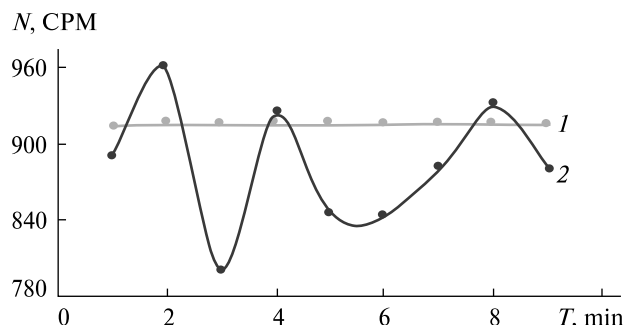


**Figure 6.** The reading of the board (line 1) and Geiger counter (line 2) after irradiation to  $\text{Co}^{60}$  with activity  $2.8 \text{ mC}$  ( $E = 1.3 \text{ MeV}$ )

fier (TL082) used in the Trans impedance amplifier (TIA) circuit with feedback resistor ( $50 \text{ k}$ ) and feedback capacitor ( $2 \text{ pF}$ ). Thirdly, the design of the peak detector designed by operational amplifier (LM358) and diode, in order to detect the output of Transimpedance amplifier (TIA). There are three LEDs in the simulation inductor to the Bpw34s output dark current. Also there is a LCD to display the output voltage of the (TIA) and (PKD). There is LCD in order to display the output voltage of the TIA and PKD voltage with the highest level of the illumination in order to define the threshold voltage value.

As a result, the diode becomes forward biased and acts as a closed switch whenever the applied voltage signal exceeds the diode’s threshold voltage. Using a diode as a buffer, the circuit operates as a buffer circuit in this case. So, whatever input is applied to the positive terminal of the op-amp, the output terminal will receive.

The diode is forward biased during the first positive half cycle of the op-amp output. Concurrently,

the capacitor is charged to the input signal's maximum peak value. The circuit is a voltage follower buffer circuit in this instance, as shown. Because the op-amp output is LOW during the first negative half cycle, the diode is biased in the other direction. As a result, the capacitor stores the maximum value of the input signal until the diode is once again forward biased. When the diode is reverse biased, the op-amp is in open loop condition and enters saturation, causing the capacitor to discharge into the R and the R to become saturated. Thus, a diminishing slope in the signal's negative cycle was occurred. The output voltage of the TIA and PK changed, and so did the maximum output current. Accordingly, the maximum output current changed with the maximum voltage. The specifications of this photodiode dosimeter read outboard are presented in the Table 2.

**3.2. Radiation Test.** Both systems are exposed to different radiation sources as listed in Table 1. The comparison between the performance of both systems are discussed in the following subsections.

**3.2.1. Irradiation with Co<sup>60</sup> with low activity 0.1 μC.** The results of exposing the Geiger counter and Bpw34s sensor board is shown in Fig. 3. The figure showed the count per minute (CPM). The photodiode sensor sensing the low-level gamma radiation of Co<sup>60</sup> with energy 2.8 MeV with low activity 0.1 μC. The Bpw34s sensor reading is saturated no significant change was observed in the reading. The Geiger counter reading is oscillated and isn't saturated. The Geiger counter is not sensitive to low dose of gamma.

**3.2.2. Irradiation with Sr<sup>90</sup> with low activity 10 μC.** The results of exposing the Geiger counter and Bpw34s sensor board is shown in Fig. 4. The figure showed the Count per Minute (CPM) and radiation accumulated

Table 2. Photodiode sensor board specifications

| Item                 | Value                           |
|----------------------|---------------------------------|
| Radiation type       | Low level gamma ray (keV – MeV) |
| Board dimension      | 10 × 10 cm <sup>2</sup>         |
| Interface            | Serial RS232                    |
| Power budget         | About 1 mW                      |
| Sampling rate        | 250 ksp/s                       |
| Sensitivity          | 19 Count/keV                    |
| Mechanical interface | Albox with dimension 16 × 17 cm |
| Weight               | 50 g without batteries          |

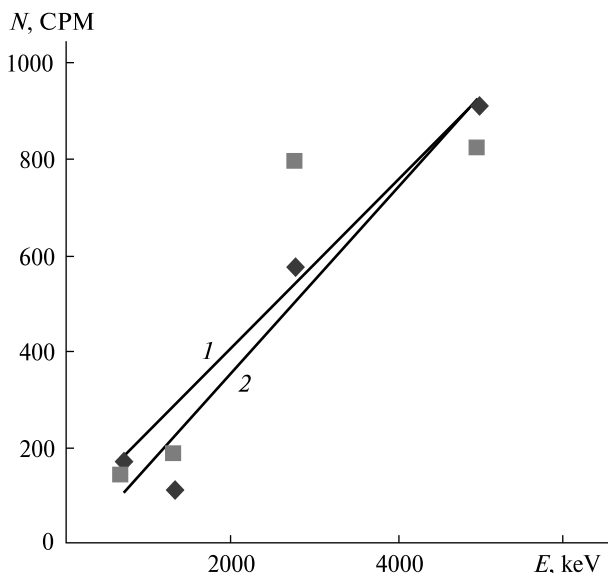


Figure 7. Sensitivity of the sensor board (diamonds, line 1:  $N = 0.1903E - 21.254$ ;  $R^2 = 0.9491$ ) vs. Geiger counter (squares, line 2:  $N = 0.1734E + 59.448$ ;  $R^2 = 0.7993$ )

dose in (μSV). The photodiode sensor sensing the low-level beta radiation of Sr<sup>90</sup> with energy 1.17 MeV with low activity 10 μC. The Bpw34s sensor reading is more stable than Geiger counter which shown a fluctuation in the reading. The sensor can sense in MeV range. The CPM and the radiation accumulated dose is increasing linearly with exposure time.

**3.2.3. Irradiation with Cs<sup>137</sup> with high activity 1 mC.** The results of exposing the Geiger counter and Bpw34s sensor is shown in Fig. 5. The figure showed the Count per Minute (CPM) and radiation accumulated dose in (μSV).

The photodiode sensor sensing the low-level beta radiation of Cs<sup>137</sup> with energy 662 keV with high activity 1 mC. The Bpw34s sensor reading is more stable than Geiger counter which shown a fluctuation in the reading. The sensor can sense in keV range. The CPM and the radiation accumulated dose is increasing linearly with exposure time.

**3.2.4. Irradiation with Co<sup>60</sup> with high activity 2.8 mC.** The results of exposing the Geiger counter and Bpw34s sensor is shown in Fig. 6. The figure showed the Count per Minute (CPM) and radiation accumulated dose in (μSV).

The photodiode sensor not sensing the high-level gamma radiation of Co<sup>60</sup> with energy 1.3 MeV with



high activity 2.8 mC. The Bpw34s sensor reading is saturated on 915 CPM. While the Geiger counter reading is fluctuation is less than at low level activation. The sensor cannot sense in the high MeV range.

**3.2.5. The system sensitivity.** In order to calculate the sensitivity ( $\delta$ ) of photodiode sensor and Geiger counter, it is defined as ratio of number counted  $n$  by sensor to the exposed radiation energy:

$$\delta = n/E.$$

The CPM for each source is counted after 10 min accumulated dose.

As shown in Fig. 7, the sensitivity of the Geiger counter is 17 CPM per mR hr<sup>-1</sup> while, the sensitivity of the Photodiode sensor is 19 CPM per mR hr<sup>-1</sup>. The sensitivity of the photodiode sensor is 17 CPM per mR hr<sup>-1</sup>, Range of energy measurement is keV to MeV. Through this project the design and implementation and testing for radiation sensor readout board based on photodiode are presented and described in details.

Appendix 2 includes the Figures, which illustrate a) software's flow chart, b) simulated circuit after testing, and c) the final output of the circuits with function generator.

#### 4. CONCLUSIONS

Through this work the design, implementation and testing for radiation photodiode sensor readout board are presented and described in details. A system consisting of a transimpedance amplifier (TIA)

and a peak detector (PKD) circuit for use with a Bpw34s PIN photodiode was developed with the goal of producing a low-cost system that can be used in the detection of low energy levels of gamma rays (via Arduino-Nano). The specifications of the system was determined, the board area is 100 cm<sup>2</sup>, the interface is Serial RS232, the power needed is 1 mW and the sampling rate is 250 ksp/s.

The performance of the system for the detection of gamma rays was determined using a Co<sup>60</sup>, Cs<sup>137</sup>, and Sr<sup>90</sup> radiation source. In comparison with Geiger counter, the photodiode reading is more stable than Geiger counter. The sensitivity of the Geiger counter is 17 % while, the sensitivity of the Photodiode sensor is 19 %. The photodiode can sense in range from keV to MeV. When the photodiode sensor exposes to Co<sup>60</sup> with high activity 2.8 mC the reading is saturated. The photodiode is more reliable at low activity. The designed circuit can work as an Beta and Gamma counter. Indeed, it could be used in a lunar mission after more space environment qualification tests.

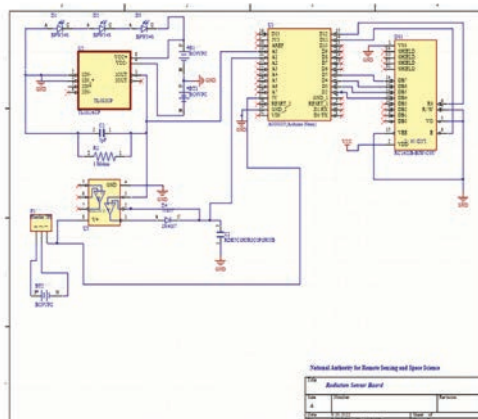
#### COMPETING INTERESTS

The authors declare that they have no known competing financial interests or personal relationships that could have appeared to influence the work reported in this paper. The data that support the findings of this study are openly available.

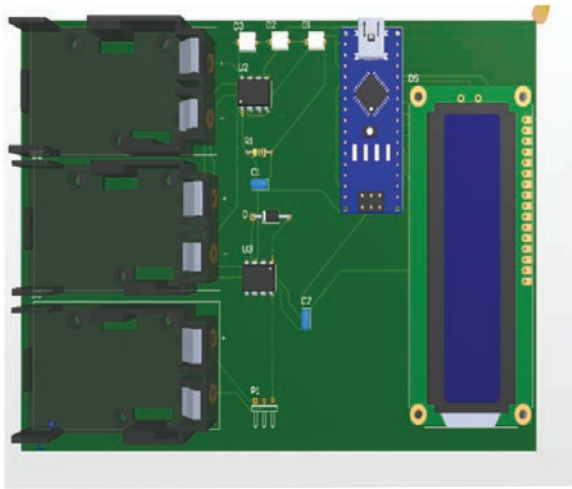
### Appendix 1



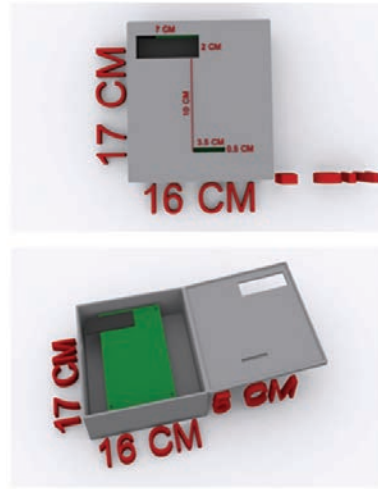
a) The prototype of the sensor board



b) The Schematic design of on the sensor board

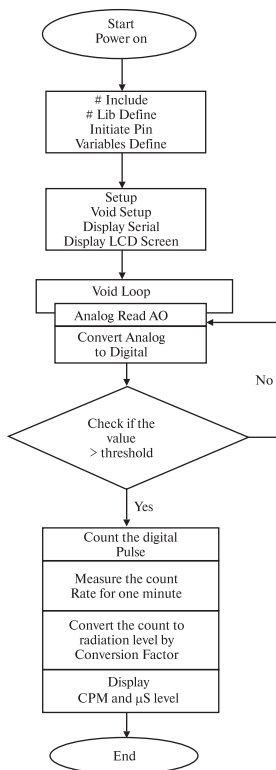


c) Final 3D design of the sensor board

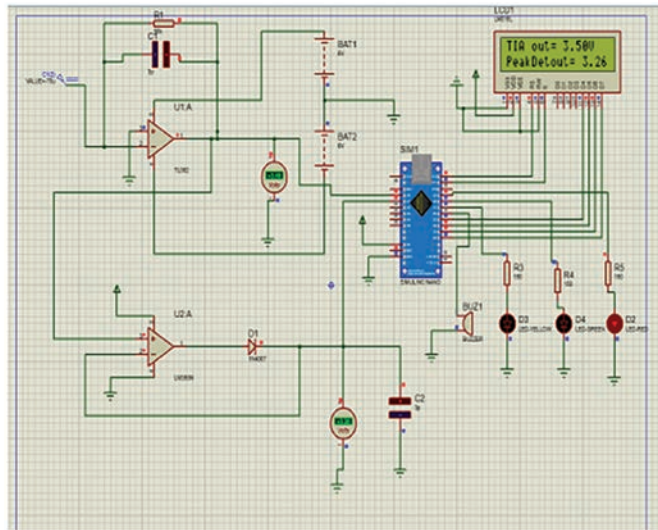


d) Mechanical structure of the aluminum box

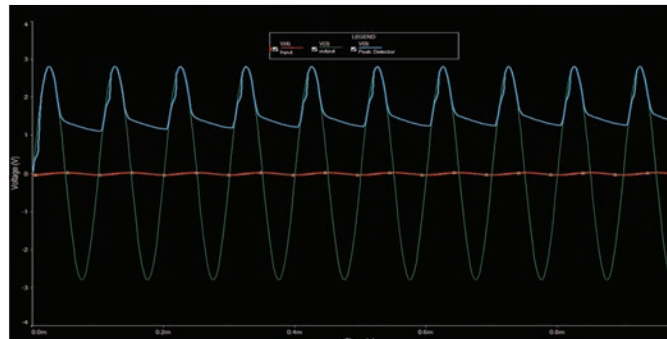
## Appendix 2



a) Software's flow chart



b) Simulated circuit after testing



c) The final output of the circuits with function generator

## REFERENCES

1. Achtenberg K., Mikolajczyk J., Szabra D., Prokopiuk A., Bielecki Z. (2020). Review of peak signal detection methods in nanosecond pulses monitoring. *Metrology and Measurement Systems*, **27**(2), 203–218. DOI:10.24425/mms.2020.132770.
2. Chierici A., Malizia A., di Giovanni D., Fumian F., Martellucci L., Gaudio P., d'Errico F. (2021). A low-cost radiation detection system to monitor radioactive environments by unmanned vehicles. *Eur. Phys. J. Plus*, **136**.
3. Gieseler J., Oleynik P. (2020). Radiation Monitor RADMON aboard Aalto-1 CubeSat: First results. *Adv. Space Res.*, **66**, 52–65.
4. Gooda P. H., Gilboy W. B. (1987). High resolution alpha spectroscopy with low cost photodiodes. *Nuclear Instrum. and Methods Phys. Res. A*, **255**, 222–224.
5. Graeme J. G. (1996). *Photodiode Amplifiers: OP AMP Solutions*, McGraw Hill Professional.
6. Knoll G. F. (2010). *Radiation Detection and Measurement*, 4<sup>th</sup> edition, Hoboken, N.J: Wiley.
7. Narici L., Berger T., Matthiä D., Reitz G. (2015). Radiation Measurements Performed with Active Detectors Relevant for Human Space Exploration. *Front Oncol.*, **5**, 273. Publ. online 2015, Dec 8. DOI: 10.3389/fonc.2015.00273.
8. Nowotny R., Reiter W. L. (1977). The use of silicon pin-photodiodes as a low-energy photon spectrometer. *Nuclear Instrum. and Methods Phys. Res. A*, **147**, 477–480.
9. Oliveira C. N. P., Houry H. J., Santos E. J. P. (2016). PiN photodiode performance comparison for dosimetry in radiology applications. *Phys. Medica*, **32**, 1495–1501.
10. Renker D., Lorenz E. (2009). Advances in solid state photon detectors. *J. Instrum.*, **4**, P04004.

Стаття надійшла до редакції 26.02.2023

Після доопрацювання 08.05.2023

Прийнято до друку 08.05.2023

Received 26.02.2023

Revised 08.05.2023

Accepted 08.05.2023

Д. Елфікі\*<sup>1</sup>, керівник відділу структурного, термічного та космічного середовища

Департаменту космічних наук, доц., проф.

ORCID: 0000-0003-4772-667X

E-mail: delfiky@narss.sci.eg

С. Азіз<sup>1</sup>, РА зі структурного, термічного та космічного середовища Департаменту космічних наук, магістр

E-mail: sara.ramadan.aiz93@gmail.com\*, sara.ramadan@narss.sci.eg\*

Н. Хешам<sup>1</sup>, РА зі структурного, термічного та космічного середовища Департаменту космічних наук, бакалавр

E-mail: nourhanhesham531@gmail.com

А. Ахмед<sup>2</sup>, нач. відділу корисного навантаження, д-р техн. наук

E-mail: ayman.ahmed@moonvillageassociation.org

<sup>1</sup>Національне управління з дистанційного зондування та наук про космос (НУДЗНК)

23, вул. Йозефа Тіто, Ель Ножа, Каїр 11769, Єгипет

<sup>2</sup>Єгипетське космічне агентство, Каїр, Єгипет

## НИЗЬКОСОБІВАРТИСНИЙ ДОЗИМЕТРИЧНИЙ МОДУЛЬ ДЛЯ МІСІЇ MVA LUNAR LANDER

Знання радіаційного середовища Місяця має вирішальне значення для майбутніх місій дослідження космосу, оскільки відсутність атмосферного та магнітного екранування супутника дозволяє зарядженим частинкам різної енергії та походження проникати на його поверхню. У дослідженнях космічного радіаційного середовища загальною практикою є використання радіаційних дозиметрів для вимірювання поглиненої дози та її потужності. У цьому дослідженні корисне навантаження включатиме радіаційний дозиметр, здатний вимірювати інтенсивність радіації на поверхні місця посадки. Концепція дизайну та реалізація системи зчитування рівня радіації для вимірювань в режимі реального часу поглиненої дози гамма-випромінювання та потужності дози на поверхні зони приземлення для місії MVA базуються на фотодіодному давачі, який є комерційно доступним і використовуватиметься як давач гамма-випромінювання. Модуль протестовано на низькому рівні радіоактивності (Cs<sup>137</sup>, Co<sup>60</sup> та Sr<sup>90</sup>). Працездатність модуля на основі фотодіода перевірено за допомогою лічильника Гейгера. Низька вартість та висока чутливість такого модуля визначення рівня радіації є його суттєвими перевагами.

**Ключові слова:** місяцехід, радіаційний дозиметр, фотодіодний сенсор, ТІА.